

# HEMT Millimeter-wave Monolithic IC Technology for 76-GHz Automotive Radar

●Yuu Watanabe ●Naofumi Okubo

(Manuscript received June 8, 1998)

**This paper describes monolithic IC technologies for developing practical automotive radar systems, covering the HEMT device structure, IC fabrication process, flip-chip assembling, and circuit design. InGaP/InGaAs HEMTs with a 0.15- $\mu\text{m}$  gate were used in millimeter-wave monolithic ICs for the W-band, providing a maximum stable gain of 9 dB at 76 GHz. Height-controlled flip-chip bonding with pillar interconnection was demonstrated as a low-cost assembly method. A de-embedding technique to model a face-down co-planar waveguide was proposed. A chip set was designed with this technique, consisting of a 76-GHz amplifier, 76-GHz mixer, 76-GHz SPDT switches, 38/76-GHz doubler, 38-GHz voltage-controlled oscillator, and 38-GHz buffer amplifier. The fabricated chip set showed high performance for automotive radar systems.**

## 1. Introduction

In line with recent advances in millimeter-wave systems based on semiconductor technology development, the application of these systems is being extended to commercial fields.<sup>1,2)</sup> One of the most promising areas is automotive radar to provide active safety for driving. Research on automotive radar started in the early 1970s in the United States. In 1981, Fujitsu developed a 50-GHz radar sensor. These efforts, however, did not meet the demands of the market due to cost and size. In the late 1980s, several national programs promoted research on millimeter-wave systems, while during the same period GaAs semiconductor manufacturing grew strongly due to the rapid spread of wireless communications. These circumstances stimulated commercial interest in millimeter-wave systems, including automotive radar.

Frequency allocation is a key to the market of any system utilizing electromagnetic waves. The Japanese Ministry of Posts and Telecommunications (MPT) assigned the 60-GHz band for low-power millimeter radar systems in 1995. Fol-

lowing the allocation of the 76-GHz band for radar in the U.S. and Europe, the MPT decided in 1997 to assign the same band to automotive radar systems in addition to the 60-GHz band. Although this action promoted a global standard for commercial use, it gave a rise to challenging technical issues.

To realize practical, reasonably priced radar systems for passenger cars, the frequency performance of the devices must be improved and costs reduced. Monolithic integration is the usual approach to cost reduction and is still important for the W-band.<sup>3)</sup> Much effort has recently been devoted to the development of monolithic integrated circuits, and it has been shown that peripheral elements play a more important role in this frequency region. Die positioning and wiring in a package seriously affect the circuit performance and yield, resulting in higher costs. Flip-chips can be used to avoid these difficulties, as well as digital circuits.<sup>4)</sup> Using flip-chip bonding, chip positioning can be automated with greater accuracy. The wafer process for flip-chips will be simpler

than that for conventional microwave devices. To make use of these advantages in millimeter-wave applications, problems associated with the short wavelength must be overcome.<sup>5),6)</sup>

This paper describes a millimeter-wave monolithic IC (MMIC) technology for the development of 76-GHz automotive radar, including a 0.15- $\mu\text{m}$  HEMT IC process, flip-chip with pillar interconnection, and W-band face-down circuit design. Using an InGaP/InGaAs/GaAs heterostructure with electron beam lithography, the HEMT exhibited good improvement compared to the conventional structure. The pillar interconnection technique was employed in the millimeter-wave monolithic IC for flip-chips. We have demonstrated the good electrical properties of the flip-chip and showed the difficulty of design due to the face-down structure. Several MMICs were successfully designed and fabricated for the 76-GHz automotive radar sensor. These face-down circuits exhibited good performance in the W-band.

## 2. Device technology

The operation frequency of 76 GHz in MMICs is challenging for transistor technology. The transistors in the circuit must provide sufficient gain at 76 GHz, which conventional semiconductor circuits have not reached. Heterojunction devices such as HEMTs have fundamental advantages over other types of transistors in terms of high-frequency performance, because of the bandgap difference in their structure. Fujitsu has already developed a 0.25- $\mu\text{m}$  gate HEMT technology using photolithography and sidewall techniques, which is commercially available for several millimeter-wave systems. However, even with quarter-micron HEMTs, the frequency performance is not sufficient for 76-GHz automotive radar systems; high-performance transistors with an  $f_{\text{max}}$  exceeding 150 GHz are required.

The reduction of gate capacitance and increase in transconductance are important to improve transistor characteristics. Scaling is the traditional approach for FET technology and is

effective for improving performance even in the sub-micron region, but parasitic factors cannot be neglected for high-performance devices. Such phenomena as the short channel effect, increase in gate resistance and fringing capacitance degrade the transistor performance.

**Figure 1** shows the new structure employed for the 0.15- $\mu\text{m}$  HEMT. The T-shaped gate was patterned by electron beam lithography. This makes the gate electrode free from the sidewall, thus reducing the fringing capacitance. The i-GaAs/i-InGaAs/n-InGaP/n-GaAs epitaxial layers were grown by MOCVD, where n-InGaP is the electron supply layer instead of the AlGaAs layer in the conventional structure. Thanks to high doping in the InGaP layer, the distance between the channel and gate can be reduced compared with the conventional AlGaAs/GaAs HEMT. This structure thus suppresses the short channel effect for fine gate lengths.

In the fabrication process, the recess region was etched after ohmic electrode formation. The Al gate electrode was aligned in the recess region with electron beam lithography and lifted off. Using Al for the T-shaped gate electrode, the gate resistance is low even for a gate length of 0.15  $\mu\text{m}$ . We optimized the structure taking account of the high frequency and process stability.

**Figure 2** shows the small-signal frequency characteristics of a 0.15- $\mu\text{m}$  HEMT with a bias condition of  $V_{\text{ds}} = 3 \text{ V}$  and  $V_{\text{gs}} = -0.4 \text{ V}$ , indicating a cut-off frequency ( $f_{\text{T}}$ ) of 90 GHz, a maximum oscillation frequency ( $f_{\text{max}}$ ) of 170 GHz, and a maxi-

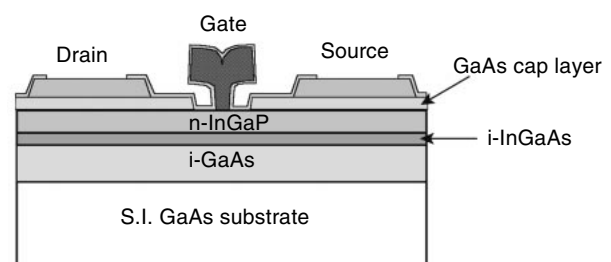


Figure 1  
InGaP/InGaAs HEMT cross sectional structure.

imum stable gain (MSG) of 9 dB at 76 GHz. Here,  $f_{\max}$  was determined from the maximum available gain curve instead of by  $-6$  dB extrapolation of the unilateral power gain curve. This result shows that the new HEMT structure effectively reduces the parasitic effects.

Using the  $0.15\text{-}\mu\text{m}$  gate HEMT, we developed an MMIC process for low-cost millimeter wave applications. Similar to the conventional MMICs, MIM capacitors, epitaxial resistors, and air bridge wiring are employed for passive elements. The conventional MMIC uses micro-strips as transmission lines, which need a ground plane on the back-side of the chip and via holes to connect the back-side ground plane to the face-side of the chip. The thickness of the chip must be precisely controlled to maintain the impedance of the transmission line. This requires a wafer thinning process and wafer penetrating process for the fabrication. The controllability of the process to determine wafer thickness and via size poses a difficult problem to produce much higher frequency circuits with the micro-strip structure. A co-planar waveguide (CPW) is often used in millimeter-wave systems and its structure is also convenient for flip-chip

assembling, since all electrodes in the circuit are placed only on one side of the chip. No wafer thinning or via penetrating process is needed for co-planar circuits. The chip can also be thick, thus retaining mechanical strength during the chip bonding process.

Digital LSIs usually use a bump technology based on transferred solder for the interconnections of flip-chips. The MMIC for the W-band requires more precise positioning and size of interconnection electrodes to avoid degradation due to impedance mismatching than digital LSIs because of its short wavelength. In order to obtain good positioning with a small diameter interconnection, we developed a pillar technique that is a part of the fabrication process. After the metallizing process for the MMIC co-planar lines, pillar-shaped electrodes with  $40\text{-}\mu\text{m}$  diameter gold are formed on the wafer by electroplating. **Figure 3** shows an SEM photograph of the MMIC, showing the

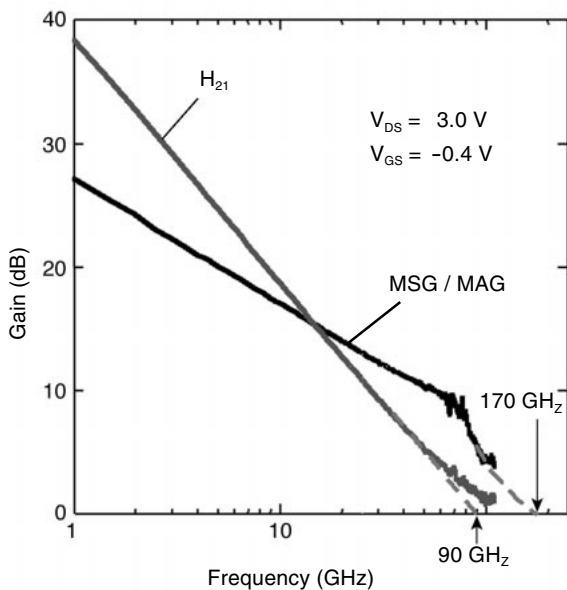


Figure 2  
0.15- $\mu\text{m}$  InGaP/InGaAs HEMT characteristics.

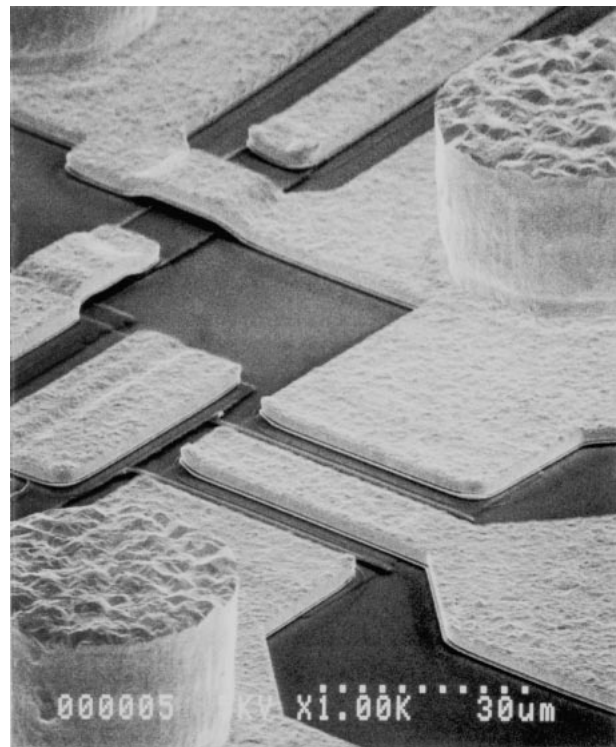


Figure 3  
SEM image of MMIC surface, showing HEMTs and pillars.

pillars, HEMTs, and an air-bridge on the circuit. This technique provides flexibility, allowing the pillars to be placed anywhere on the chip and thus reduces the source inductance of each transistor by placing a grounded connection just beside the devices. In the fabrication process, pillar plating is also needed, instead of wafer thinning, back-side alignment, via hole etching, and back-side plating, which are conventionally used in MMICs. The entire process is thus simplified with this pillar technique.

### 3. Flip-chip technology for millimeter-wave devices

The importance of assembling is much larger for high-frequency applications than for digital or low-frequency ones. The physical length of packages seriously affects the performance of MMICs because the wavelength is comparable to the dimensions of the package and leads. Flip-chip bonding causes little loss in performance or size reduction, and its assembly precision enables low-cost fabrication.<sup>7-9)</sup> However, two problems remain. Firstly the transmission line to the substrate exerts a proximity effect on the high-

frequency characteristics of the device. Secondly, the reliability of the lines may be compromised when subjected to thermal and mechanical stresses inherent in the inflexible structure of flip-chip bonding. We investigated the high-frequency characteristics and reliability of the flip-chip bonding portion between a GaAs chip and alumina substrate.

The gold-tin eutectic reaction method was employed for flip-chip bonding, in which the chip and substrate were heated after connecting the gold pillars on the chip to the tin of the substrate. This process potentially causes less damage to the fragile GaAs chips than conventional gold-to-gold thermocompression bonding<sup>7,8)</sup> because of its lower temperature and lower load. In addition, the gold-tin method avoids solder contamination of the gold transmission line on the chip, which can be a problem in the solder-bump bonding method.<sup>9)</sup>

The test piece consisted of a 2-mm-square GaAs chip with gold CPW lines and gold pillars on one surface, and a 10-mm-square 0.65-mm-thick alumina substrate with a patterned thin film metallization on its surface. **Figure 4** shows a schematic diagram of our flip-chip. The substrate metallization consists of 100 nm of Ti, 3,000 nm of Cu, and 500 nm of Sn. The chip was mounted on the substrate with a pulse-heat tool at 350°C for 10 seconds under a 20 g/pillar load.

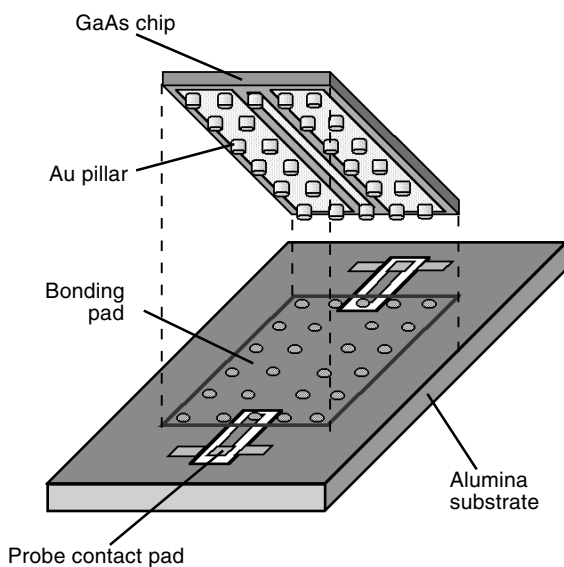


Figure 4  
Flip-chip for pillar interconnection.

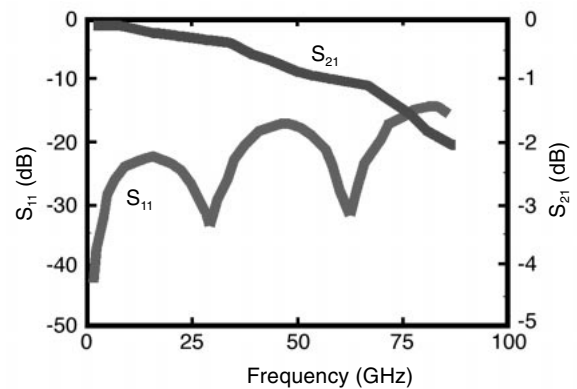


Figure 5  
Scattering parameters for flip-chip bonded transmission line.

**Figure 5** shows the scattering parameters of the sample: S21 at 76 GHz measures -1.8 dB. By removing the return loss (-0.3 dB), the loss from the substrate coplanar lines (-0.5 dB) and the transmission line on the chip (-0.6 dB), the insertion loss of the pillar portion is estimated to be -0.2 dB/pillar. S11 is below -15 dB at 76 GHz. Using simulation, typical values for conventional wire bonding were estimated at -0.6 dB for S21, and -10 dB for S11.<sup>3)</sup> These results show that flip-chip bonding has both a lower insertion loss and a return loss than conventional wire bonding.

Next, we estimated the proximity effect on the high-frequency characteristics of the device by simulating the electromagnetic field using the moment method. **Figure 6** shows the simulated characteristic impedance of the transmission line on the chip as a function of the pillar height. The transmission line on the chip has a coplanar structure for a 20- $\mu\text{m}$  gap and 20- $\mu\text{m}$  line width. The characteristic impedance gradually decreases with a decrease in pillar height. A  $\pm 5\text{-}\mu\text{m}$  change in the height of a 20- $\mu\text{m}$ -high pillar results in a  $\pm 2\text{-}\Omega$  change in the 52- $\Omega$  characteristic impedance. The slope of the curve becomes remarkable below a 15- $\mu\text{m}$  pillar height. This is possibly explained by the change in the transmission mode. The result indicates that the flip-chip needs bonding technology with a controlled air gap, especial-

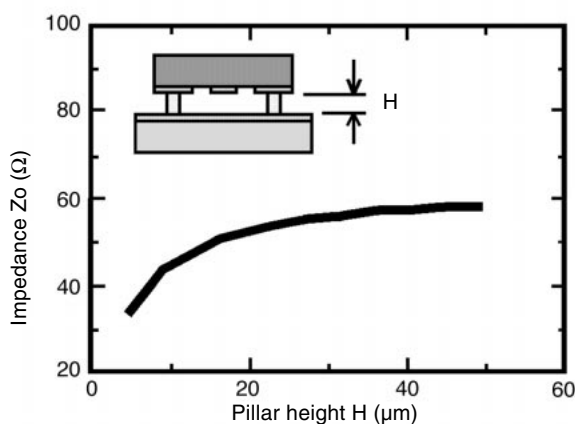


Figure 6  
Effect of pillar height on characteristic impedance of chip coplanar waveguide.

ly at a low pillar height such as 10  $\mu\text{m}$ . The controllability closely depends on the load in the bonding process. Gold-tin eutectic bonding is suitable because of its low load.

The pillar adherence strength was determined by measuring the die shear strength of the flip-chipped GaAs chips. The pillar adherence strength was equivalent to or larger than the TAB bump adherence strength.<sup>7)</sup>

In general, the major problem in flip-chip bonding is the thermal expansion mismatch between the chip and substrate, because both are inflexible and thermal stress concentrates at the bonding portion. GaAs has a thermal expansion coefficient (6.0 ppm/ $^{\circ}\text{C}$ ) similar to that of alumina (6.5 ppm/ $^{\circ}\text{C}$ ), which is a typical substrate material. The flip-chip bonding of GaAs devices on an alumina substrate is expected to have a relatively small thermal expansion mismatch. The bonding reliability was estimated by thermal cycle tests (-55 to 150 $^{\circ}\text{C}$ ; 1,000 cycles), thermal shock tests

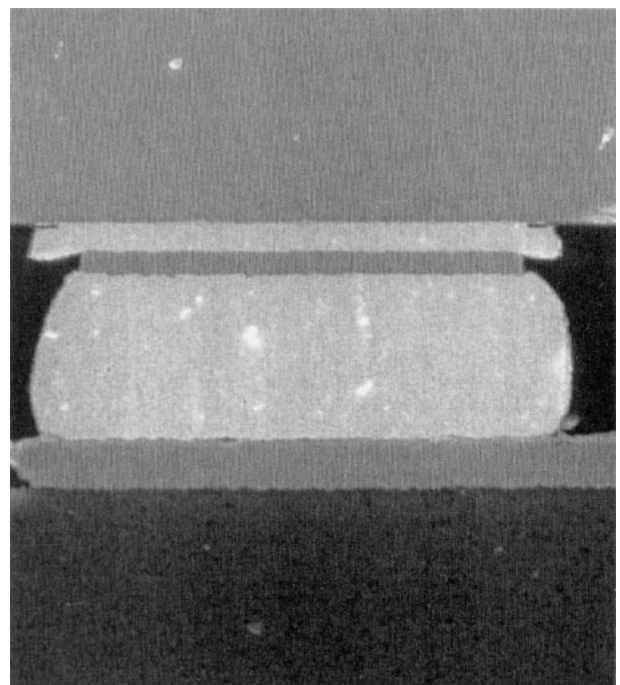


Figure 7  
SEM cross section of Au-Sn bonded pillar. From top: GaAs chip, metallized layer on chip, pillar, pad on substrate, and alumina substrate.

(0 to 100°C; 1,000 cycles) and vibration tests (10 to 200 Hz; 10 G, 6 hours). All samples passed these tests, indicating that the bonding technology has a high reliability. **Figure 7** shows a cross-section of the flip-chip bonding after the thermal cycle test.

## 4. Circuit Design

### 4.1 Face-down chip design

Designing the W-band millimeter-wave circuit with face-down chips is another challenge. A precise model of the transmission line is one of the key issues for MMICs. In spite of much research on CPW design,<sup>10),11)</sup> there remain several difficulties in using CPW for flip-chip circuits, such as the proximity effect and signal transition to the chip. An actual flip-chip CPW line contains signal transition parts such as pillars or bumps to transmit a signal from the external feed line to the CPW line. When characterizing the actual CPW lines, however, the signal transition part hinders the de-embedding of the external feed lines since the transverse electromagnetic field extends toward each line. **Figures 8(a) and (b)** show a portion of an actual flip-chip structure, which includes a signal transition pillar. A simulated result of a magnitude contour map shows the electric field distribution at a distance of 10 μm from the alumina substrate at 76 GHz. The simulation was performed using a 3-dimensional

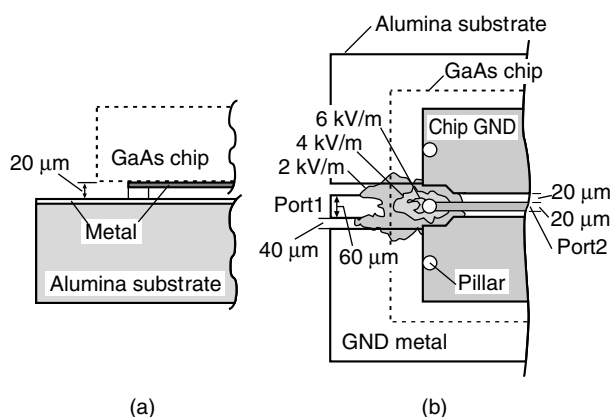


Figure 8  
Electromagnetic field simulation for flip-chip coplanar waveguide. (a) Side view of analyzed structure, (b) Top view of electromagnetic field distribution around signal transition pillar at 76 GHz.

full-wave electromagnetic field simulator. As shown in Figure 8(b), the electric field expands under the CPW line on the GaAs chip. This leads to interaction between the signal transition pillar and CPW line, thus making it difficult to determine the reference plane when de-embedding each line.

When designing the circuits, the pillar transitions and CPW lines must be characterized independently. Therefore, we propose an experimental technique to model flip-chip CPW lines without signal transition pillars. This experiment is based on the reversed-structure flip-chip, which consists of a CPW line chip and lid ground. The CPW lines are measured with the lid ground attached to the pillar. By using this technique, the characteristics of the transmission line can be evaluated without affecting signal transition through the pillars. We obtained that  $Z_0 = 49.0$  ohms,  $E_{\text{eff}} = 5.41$ , and  $A_{\text{ttn}} = 0.300$  dB/mm from measured data for a line width of 20 μm, a ground-to-ground spacing of 60 μm, and a pillar height of 20 μm. We also obtained that  $Z_0 = 55.9$  ohms,  $E_{\text{eff}} = 6.33$ , and  $A_{\text{ttn}} = 0.241$  dB/mm for the same line width and ground-to-ground spacing for a line without the lid ground. As mentioned in the previous section, the CPW line and ground on the substrate interact. These results closely agree with the simulation results and indicate that W-band flip-chip MMICs with CPW lines can be designed using the quasi-TEM mode approximation. Thus, we identified the parameters for the transmission line model in the circuit simulator by using this method.

### 4.2 MMIC chip set for automotive radar

Based on the CPW model, we developed a 76-GHz chip set for automotive radar. The chip set consists of a 76-GHz amplifier, 76-GHz mixer, 76-GHz SPDT switches, 38/76-GHz doubler, 38-GHz voltage-controlled oscillator, and 38-GHz buffer amplifier. **Figure 9** shows photographs of the chip set.

The amplifier has a two-stage configuration

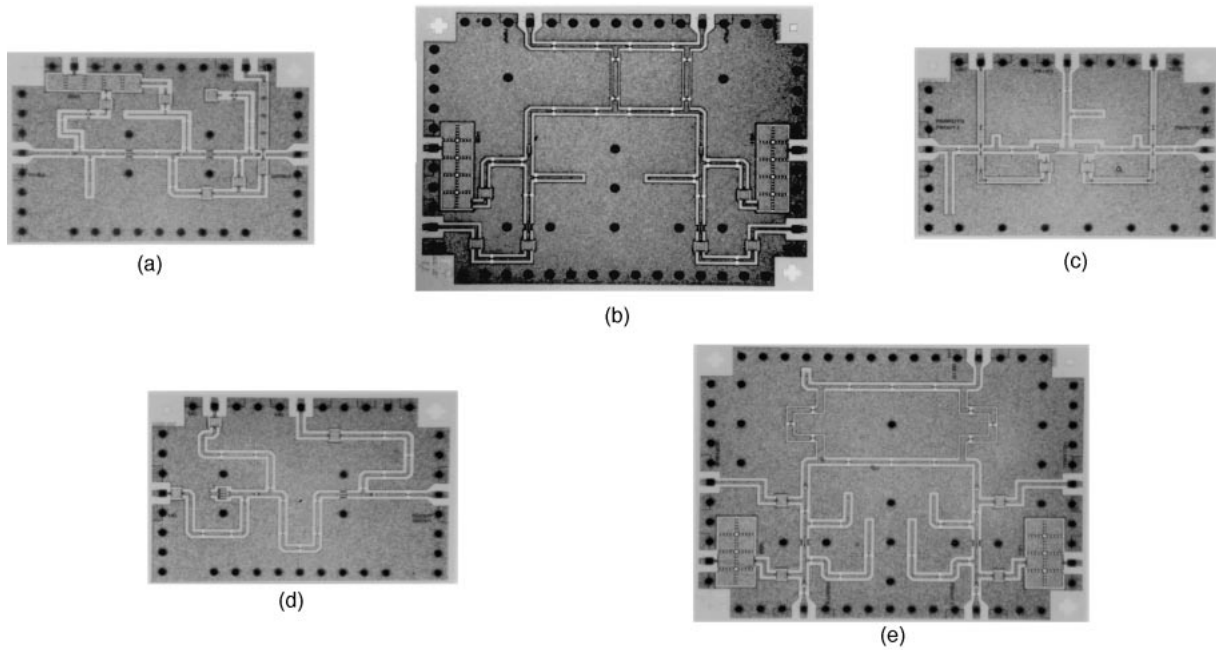


Figure 9 Photographs of 76-GHz MMIC chip set (a) 76-GHz amplifier, (b) 76-GHz mixer, (c) 76-GHz SPDT switch, (d) 38/76-GHz doubler, (e) 38-GHz voltage-controlled oscillator and 38-GHz buffer amplifier.

with 80- $\mu\text{m}$  HEMTs. Short-circuited stubs are used in the inter-stage and output matching circuits to reduce the chip size. Each short-circuited stub is composed of a transmission line and a grounded MIM capacitor. **Figure 10** shows the measured S-parameters of the amplifier. The amplifier has a small-signal gain of 10.6 dB at 76.5 GHz.

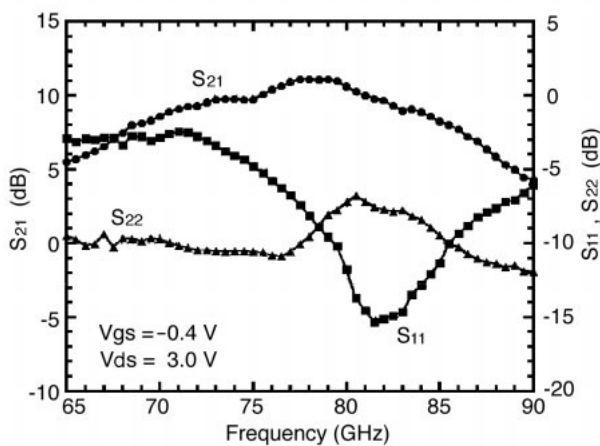


Figure 10 Measured characteristics of 76-GHz 2-stage amplifier.

The mixer has a singly balanced configuration. The RF and LO signals are fed into the gate of each HEMT through the  $0-\pi$  hybrid circuit. The  $0-\pi$  hybrid circuit consists of a quarter-wavelength transmission line and a branch line hybrid circuit. The mixer using the  $0-\pi$  hybrid circuit exhibits good isolation between the RF and LO ports even if the unit mixers have large reflection coefficients. Also, the mixer reduces AM noise from the LO in cooperation with an external IF 180-degree hybrid circuit. The mixer has a conversion gain of -4 dB at a 76-GHz LO frequency for an LO power of -1 dBm.

The 76-GHz SPDT switch consists of two parallel-resonated 160- $\mu\text{m}$  HEMTs. The transmission line connected to the drain and source terminals of the HEMT is employed as a resonant inductor in parallel with the fringing capacitance. The obtained insertion loss and isolation at 76.5 GHz were 3.4 dB and -17 dB, respectively.

The 38/76-GHz doubler chip consists of two single-ended 80- $\mu\text{m}$  HEMT frequency doublers and a branch line hybrid circuit. This circuit con-

figuration leads to a low input return and high isolation between the two output ports. **Figure 11** shows the measured frequency response of the doubler. The doubler has a conversion gain of -3.7 dB for a 38.25-GHz input signal power of 3 dBm.

In the 38-GHz voltage controlled oscillator, we adopted the reverse channel HEMT configuration to generate sufficient negative resistance and reduce the size of the source feedback circuit. The oscillator uses the transmission line resonator terminated by a 160- $\mu\text{m}$  Schottky-barrier diode as a varactor. The 38-GHz buffer amplifier provides impedance isolation between the oscillator and the external load. The chip has an output power of -0.7 dBm at 39.6 GHz.

**Figure 12** shows an SEM photo of the flip-chip MMIC, indicating the amplifier chip on the evaluation board.

## 5. Conclusion

We have successfully developed an HEMT MMIC technology for 76-GHz automotive radar. The wafer process is based on a 0.15- $\mu\text{m}$  InGaP/InGaAs HEMT and interconnecting pillars for flip-chip bonding. The maximum stable gain of the

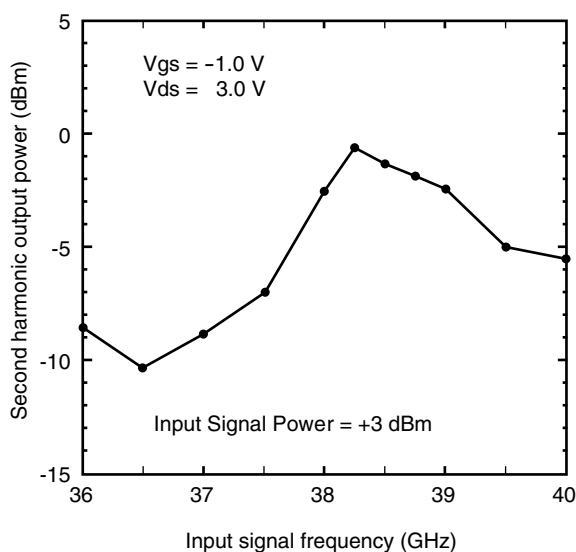


Figure 11 Measured frequency response of 38/76-GHz doubler.

HEMT is 9 dB at 76 GHz. The flip-chip bonding technology uses gold micro pillars and tin metallization on an alumina substrate. Results of reliability tests indicated that the flip-chip bonding is very resistant to thermal and mechanical stresses, and thus is suitable for practical use. For designing flip-chip mounted MMICs for the W-band, we propose an experimental method to model face-down CPW transmission lines. By using this model, the chip set was designed and fabricated, and achieved sufficient performance for 76-GHz automotive radar systems. The results indicated that our MMIC technology is promising for achieving low-cost 76-GHz automotive radar systems.

## References

- 1) H. H. Meinel: Commercial Applications of Millimeter Waves; History, Present Status, and Future Trends. IEEE Trans. MTT, **43**, 7, p.1639 (1995).
- 2) N. Okubo: Millimeter-wave Automotive Radar. MWE'96 Microwave Workshop Digest, pp.370-375, 1996.
- 3) Y. Watanabe and N. Okubo: Millimeter-wave

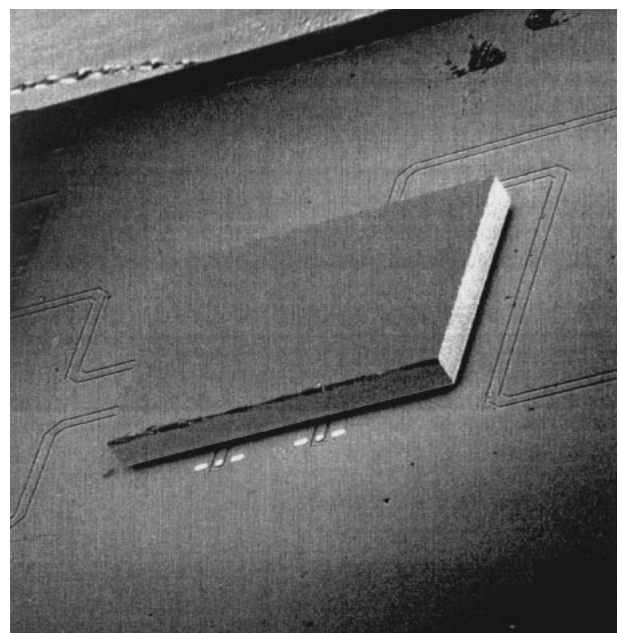


Figure 12 SEM photograph of flip-chip MMIC.



Monolithic IC Technology for 60-GHz Application. 1997 International Conference on GaAs Manufacturing Technology, pp.54-57, 1997.

- 4) S. Aoki, H. Someta, S. Yokokawa, K. Ono, T. Hirose and Y. Ohashi: A Flip Chip Bonding Technology Using Gold Pillars For Millimeter-wave Applications. IEEE MTT-S IMS Digest, pp.731-734, 1997.
- 5) T. Hirose, K. Makiyama, T. M. Shimura, S. Aoki, Y. Ohashi, S. Yokokawa, and Y. Watanabe: A Flip-Chip MMIC Design with CPW Technology in the W-band. IEEE MTT-S IMS Digest, pp.525-528, 1998.
- 6) T. Shimura, Y. Kawasaki, Y. Ohashi, K. Shirakawa, T. Hirose, S. Aoki, H. Someta, K. Makiyama, and S. Yokokawa: 76GHz Flip-chip MMICs for Automotive Radars. IEEE RFIC Symp. Digest, pp.25-28, 1998.
- 7) T. Krems, W. Haydl, H. Massler, and J. Rudiger: Millimeter-wave Performance of Chip Interconnections using Wire Bonding and Flip Chip. 1996 IEEE MTT-S IMS, pp.247-250, 1996.
- 8) H. Sakai, Y. Ota, K. Inoue, T. Yoshida, K. Takahashi, S. Fujita, and M. Sagawa: Millimeter-wave ICs using Flip-Chip Bonding Technology. MWE 95 Microwave Workshop Digest, pp.311-316, 1995.
- 9) G. Bauman, D. Ferling, and H. Richter: Comparison of flip-chip and wire bond interconnections and the technology evaluation on 51 GHz transceiver modules. 26th EuMC Digest, p.98, 1996.
- 10) W. H. Haydl, L. Verweyen, T. Jakobus, M. Newumann, A. Tessmann, T. Krems, M. Schlechtweg, W. Rinert, H. Massler, J. Rudiger, W. Bronner, A. Hulsmann, and T. Fink: Compact Monolithic Coplanar 94 GHz Front Ends. IEEE MTT-S Digest, pp.1281-1284, 1997.
- 11) Rick Sturdivant: Reducing the Effects of the Mounting Substrate on the Performance of GaAs MMIC Flip Chips. IEEE MTT-S Digest, pp.1591-1594, 1995.



**Yuu Watanabe** received the B.S. and M.E. degrees from Kyoto University, Kyoto, Japan in 1980 and 1982, respectively, and the Ph.D. degree from Osaka University, Osaka, Japan in 1997. In 1982 he joined Fujitsu Laboratories Ltd., where he has been engaged in the research and development of heterostructure devices. He is a member of the Institute of Electrical and Electronics Engineers and the Institute of Electronics,

Information and Communication Engineers of Japan.



**Naofumi Okubo** received the B.E. and M.E. degrees from Niigata University, Niigata, Japan in 1976 and 1978, respectively. In 1978 he joined Fujitsu Laboratories Ltd., where he was engaged in the research and development of microwave and millimeter wave components and systems. He is currently a senior researcher at the Wireless Communication Systems Laboratory, and a member of the Institute of Electronics,

Information and Communication Engineers.